

# Single-Atom Pt<sup>+</sup> Derived from the Laser Dissociation of a Platinum Cluster: Insights into Nonoxidative Alkane Conversion

Zheyi Liu,<sup>#</sup> Zhimin Li,<sup>#</sup> Guanna Li,<sup>#</sup> Zhipeng Wang, Can Lai, Xiaolei Wang, Evgeny A. Pidko, Chunlei Xiao,<sup>\*</sup> Fanjun Wang,<sup>\*</sup> Gao Li,<sup>\*</sup> and Xueming Yang

Cite This: *J. Phys. Chem. Lett.* 2020, 11, 5987–5991

Read Online

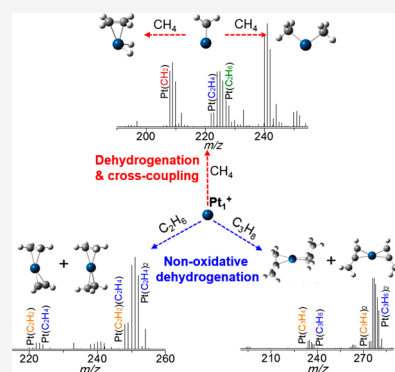
ACCESS |

Metrics & More

Article Recommendations

Supporting Information

**ABSTRACT:** In this study, we construct a 193 nm ultraviolet laser dissociation high-resolution mass spectrometry (HRMS) platform to produce Pt<sup>+</sup> cations with high efficiency, which is in situ applied for monitoring the “Pt<sup>+</sup> + alkanes” reactions (where alkanes include methane, ethane, and propane). The conversion intermediates and products could be accurately determined by an orbitrap detector with high resolution (up to 150 000). Importantly, methane conversion by Pt<sup>+</sup> cations yields [Pt + ethane]<sup>+</sup> and [Pt + ethylene]<sup>+</sup> as the sole products formed via the cross-coupling reaction of the Pt-CH<sub>2</sub> intermediate with gaseous methane. However, the Pt<sup>+</sup> cations promote only the nonoxidative dehydrogenation of ethane and propane to give the corresponding [Pt + alkenes]<sup>+</sup> and [Pt + alkynes]<sup>+</sup>. The details of the reaction mechanism are corroborated by density functional theory (DFT) calculations. These results highlight the power of HRMS with the laser dissociation of metal clusters in the generation and reaction characterization of metal ions.



C–H activation is an important topic of contemporary chemistry and catalysis stimulated by the challenging inertness of hydrocarbons and the substantial industrial interest in utilizing natural gas resources as an energy vector to replace crude oil for the production of high-value chemicals and fuels (such as light olefins).<sup>1,2</sup> Since the discovery in the 1980s, the activation and dehydrogenation of methane over “bare” sixth-row transition-metal cations M<sup>+</sup> (where, M = Ta, W, Os, Ir, Pt) in a stoichiometric manner to give the corresponding M(CH<sub>2</sub>)<sup>+</sup> carbene species (M<sup>+</sup> + CH<sub>4</sub> → M(CH<sub>2</sub>)<sup>+</sup> + H<sub>2</sub>) have been developed.<sup>3–8</sup> A wealth of thermochemical experiments have been carried out by using the techniques of guided ion beam (GIB) instruments coupled with a Fourier transform ion cyclotron resonance mass spectrometer (FT-ICR MS) in the “M<sup>+</sup> + CH<sub>4</sub>” reactions.<sup>4,5,9–11</sup> Most of the investigations of “M<sup>+</sup> + CH<sub>4</sub>” reactions have been studied under single or nearly single collision conditions within the ion cyclotron traps, and the GIB machines usually utilize metal block as the precursor for the generation of metal cations. However, the construction and operation of these sophisticated GIB-FT-ICR MS platforms are still challenging,<sup>12,13</sup> and the transient reaction intermediates are difficult to unambiguously identify.

Another challenging issue of alkane conversion by metal cations is how to rationalize the reaction mechanism,<sup>14,15</sup> as the previous experiments of the “Pt<sup>+</sup> + CH<sub>4</sub>” reaction were studied at thermo energies.<sup>16</sup> The insertion of the Pt<sup>+</sup> into one C–H bond of methane and another alkane was postulated to be the initial step by ab initio calculations,<sup>4</sup> which has not been fully confirmed by the experiments yet due to the limitation of

in situ characterization techniques and the inefficiency of Pt<sup>+</sup> cation generation. Furthermore, the intrinsic reaction mechanisms of alkane conversion are also not well identified, which requires the combined investigations of advanced experimental techniques with atomic-level theoretical approaches.<sup>17</sup>

In situ MS technology is a universal tool for the characterization of various types of species (e.g., reaction intermediates) with high detection throughput and sensitivity.<sup>18–22</sup> Besides, ultraviolet photodissociation (UVPD) was widely utilized for the fragmentation and characterization of biological molecules such as proteins, peptides, and lipids.<sup>23–26</sup> Herein, single-atom Pt<sup>+</sup> is generated in situ within the dissociation cell of an orbitrap HRMS system via the pulsed (3 Hz) ArF laser (193 nm) dissociation of ligand-protected Pt<sub>n</sub> cluster (n = 4–15) precursors, and alkanes (methane, ethane, and propane) conversion over so-formed Pt<sup>+</sup> cations can be monitored directly in the HRMS system (Scheme 1). Both the HRMS characterization results and DFT calculations verified that the methane conversion occurred by the CH<sub>4</sub> dehydrogenation and subsequent coupling processes of the so-produced [PtCH<sub>2</sub>]<sup>+</sup> intermediates with a second CH<sub>4</sub> molecule, while only the dehydrogenation processes were

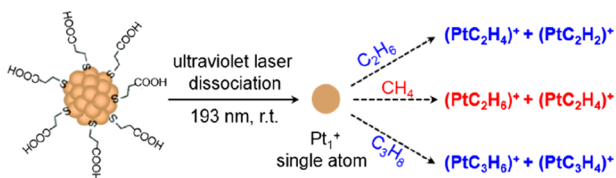
Received: May 9, 2020

Accepted: July 7, 2020

Published: July 7, 2020



**Scheme 1. Schematic Representation of Pt<sup>+</sup> Cations Generated via 193 nm Ultraviolet Laser Dissociation of the Pt Clusters for Pt<sup>+</sup> + Alkanes Conversion<sup>a</sup>**



<sup>a</sup>Methane, ethane, and propane.

found in the cases of nonoxidative ethane and propane conversion. To the best of our knowledge, this is the first time that a laser dissociation HRMS system was applied to the single-atom metal ion generation and characterization of the alkane conversions over the in situ-generated Pt<sup>+</sup> cations.

The ligand-protected Pt clusters were synthesized via our previous method.<sup>27</sup> HRMS analysis showed that these small Pt clusters are a successive distribution of Pt<sub>4–15</sub> (Figure S1a). Then, these clusters are completely dissociated to generate the Pt<sup>+</sup> cations under a 5 ns single shot of pulsed 193 nm laser irradiation (3 Hz) within the dissociation cell filled with about 20 mTorr N<sub>2</sub> gas (details in the experimental section). All of the protecting organic ligands (mercaptopropionic acid) were completely detached, and the Pt<sub>x</sub> kernel was disassembled to generate the Pt<sup>+</sup> cations during the dissociation process (i.e., Pt<sub>x</sub>(SC<sub>2</sub>H<sub>4</sub>COOH)<sub>y</sub><sup>+</sup> → Pt<sup>+</sup> + other fragments). Of note, the Pt<sup>+</sup> species can be generated only in the gas phase rather than in a supported catalyst, which is strongly evidenced by the observation of the unique isotopic pattern of Pt<sup>+</sup>, including the five stable isotopes (<sup>192</sup>Pt, <sup>194</sup>Pt, <sup>195</sup>Pt, <sup>196</sup>Pt, and <sup>198</sup>Pt) with the relative ratio 0.78:32.86:33.78:25.21:7.36 (Figure 1). And the Pt<sup>0</sup> species also are generated under laser dissociation, which cannot be detected in the mass spectra. The high mass resolution and accuracy of MS detection as well as the

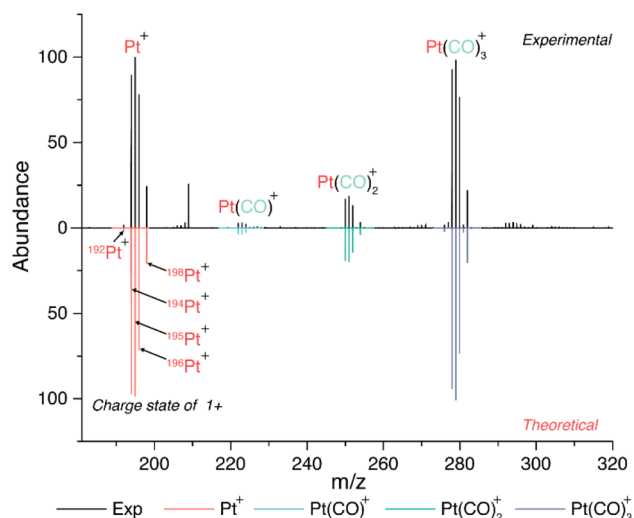


**Figure 1.** Theoretical and experimental MS spectra of the CO adsorption over the Pt<sup>+</sup> cation generated via a single-shot ultraviolet laser irradiation lasting 5 ns with about 300 ms interval. Detection conditions: *T* = 298 K, *P* = 20 mTorr, 1 vol % CO, 99 vol % N<sub>2</sub>, pulsed 193 nm laser with 1–2 mJ and a diameter of ~2 mm, and 3 Hz. The charge states of all of the detected species are +1 as determined by the mass intervals among isotopic peaks.

distribution patterns of isotopic profiles could guarantee the accurate determination of the conversion of intermediate ions. The experimentally obtained spectrum of the Pt<sup>+</sup> cation could well match its theoretical pattern of monovalent isotopic peaks with a mass error of less than 5 ppm ( $\Delta m = 0.001$  Da) (Figure S2). No other charge state of the Pt species was observed. It is worth noting that the Pt<sup>+</sup> cations cannot be directly generated in the HRMS system via the electrospray ionization of an inorganic Pt complex such as H<sub>2</sub>PtCl<sub>6</sub> even if under ultraviolet laser irradiation. As the irradiation laser shot lasted only 5 ns and highly abundant N<sub>2</sub> gas (20 mTorr) was used to fill the dissociation cell, the generated Pt<sup>+</sup> cations could be feasibly cooled for the alkane adsorption and conversion reactions. The reaction gas reagents (0.2 mTorr, partial pressure) were introduced into the dissociation cell of HRMS for Pt<sup>+</sup> conversion for about 100 ms. The reaction intermediates adsorbed onto the Pt<sup>+</sup> can immediately transfer into the orbitrap detector in about 10 ms for high-throughput monitoring before the next laser shot arrives (Scheme S1). Thus, this novel strategy is extremely suitable for the highly sensitive monitoring of short-lifetime intermediates.

Figure 1 shows that four sets of mass peaks are found in the mass range of 180 to 350 *m/z* when CO gas reagent is introduced. The mass peaks of *m/z* 194.96491, 222.95971, 250.95412, and 278.94952 can be assigned to the Pt<sup>+</sup>, [Pt(CO)<sub>1</sub>]<sup>+</sup>, [Pt(CO)<sub>2</sub>]<sup>+</sup>, and [Pt(CO)<sub>3</sub>]<sup>+</sup> species, respectively, with mass errors of less than 2 ppm (Table S1). Noticeably, the distribution patterns of the isotopic peaks suggest that all of these species are positively charged with a valence state of +1 and no other adsorption species is observed (Figure S1b). The maximum chemo-adsorption of CO molecules on the bare Pt<sup>+</sup> is three, forming a planar construction. The [Pt(CO)<sub>3</sub>]<sup>+</sup> species should be rather stable, as its abundance is the highest in the gas phase. These results demonstrate that the ultraviolet laser dissociation–HRMS platform is highly efficient for generating and characterizing the Pt<sup>+</sup> cations and conversion species.

Then, the ultraviolet-laser-generated Pt<sup>+</sup> cations are exploited for nonoxidative methane conversion. As shown in Figure 2a, five conversion species were confidently characterized with all of the isotopic peaks' baseline separated, and a mass resolution of up to 150 000 was achieved. The high mass resolution and accuracy of HRMS solved the problem of isotopic peak overlaps caused by the complex isotopic distributions of Pt-containing species, which guaranteed the assignment confidence of conversion species [Pt(CH<sub>2</sub>)<sup>+</sup>, [Pt(C<sub>2</sub>H<sub>4</sub>)<sup>+</sup>, [Pt(C<sub>2</sub>H<sub>6</sub>)<sup>+</sup>, [Pt(CH<sub>2</sub>)·H<sub>2</sub>O]<sup>+</sup>, and [Pt(C<sub>2</sub>H<sub>4</sub>)·H<sub>2</sub>O]<sup>+</sup> (Figure 2a and Table S1). As shown in Figure 2b,c, the isotopic peaks of [<sup>198</sup>Pt(C<sub>2</sub>H<sub>4</sub>)<sup>+</sup>, [<sup>196</sup>Pt(C<sub>2</sub>H<sub>6</sub>)<sup>+</sup>, and [<sup>194</sup>Pt(C<sub>2</sub>H<sub>4</sub>)·H<sub>2</sub>O]<sup>+</sup> are all well separated and unambiguously characterized, even if there is only about a 0.01 Da mass difference peaks. Intriguingly, two conversion intermediates (i.e., [Pt(CH<sub>2</sub>)<sup>+</sup> and [Pt(CH<sub>2</sub>)·H<sub>2</sub>O]<sup>+</sup>) with high stability are clearly detected, which might be generated via the dehydrogenation process of Pt<sup>+</sup> + CH<sub>4</sub> → Pt(CH<sub>2</sub>)<sup>+</sup> + H<sub>2</sub>. These similar conversion species were also found in the Au<sub>2</sub><sup>+</sup> system.<sup>28</sup> Furthermore, two conversion products (C<sub>2</sub>H<sub>4</sub> and C<sub>2</sub>H<sub>6</sub>), which chemo-adsorbed on the Pt<sup>+</sup> cations in the form of Pt(C<sub>2</sub>H<sub>4</sub>)<sup>+</sup> and Pt(C<sub>2</sub>H<sub>6</sub>)<sup>+</sup>, are also observed, which are proposed to be formed by the cross C–C coupling reaction of the C1 intermediates (vide infra). Ethylene is found to be the major product during the methane conversion over Pt<sup>+</sup>, and no

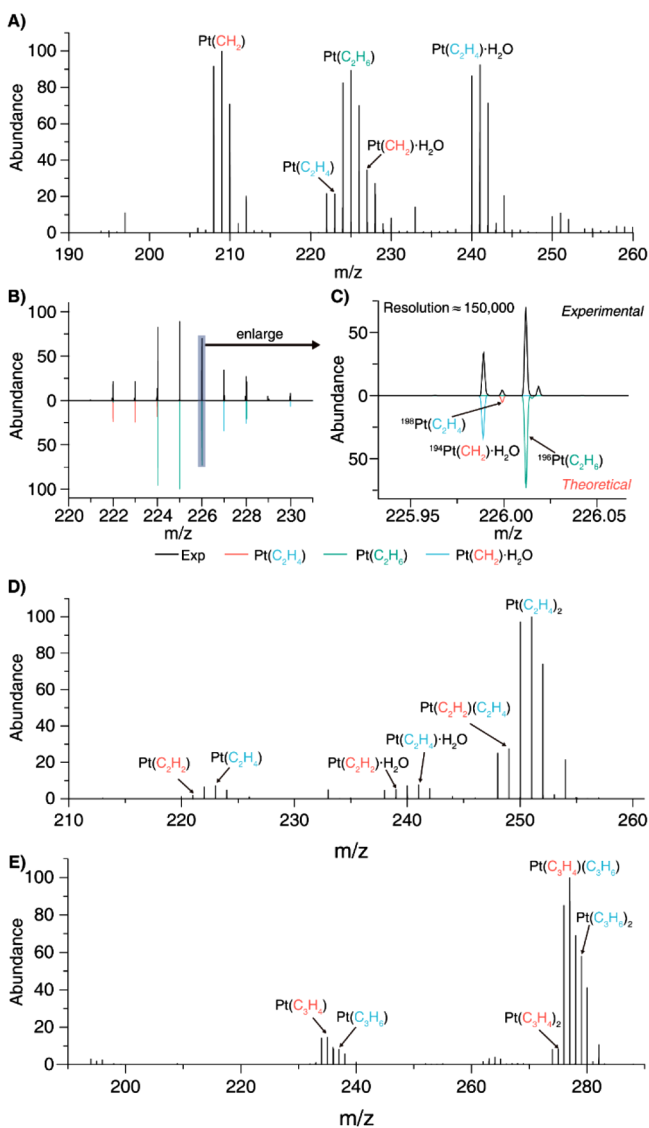


**Figure 2.** In situ HRMS monitoring of the formed  $\text{Pt}^+$  cations in the presence of alkane gases (A) methane [(B, C) with enlarged spectra of methane conversion intermediates], (D) ethane, and (E) propane. Reaction conditions:  $T = 298 \text{ K}$ ,  $P = 20 \text{ mTorr}$ , 1 vol % alkane, 99 vol %  $\text{N}_2$ , pulsed 193 nm laser with 1–2 mJ and a diameter of  $\sim 2 \text{ mm}$ , and 3 Hz (5 ns pulse width with about a 300 ms interval). No collision energy was applied to the  $\text{Pt}^+$  species during the whole alkane conversion process.

other species is observed in the wide mass range analysis (Figure S3).

Next, regarding the nonoxidative conversion of ethane and propane over the  $\text{Pt}^+$  cations, the HRMS characterizations are carried out under identical conditions. As could be seen in Figure 2d, several new species are detected by in situ HRMS characterization when ethane is introduced, which can be assigned to  $[\text{Pt}(\text{C}_2\text{H}_2)]^+$ ,  $[\text{Pt}(\text{C}_2\text{H}_4)]^+$ ,  $[\text{Pt}(\text{C}_2\text{H}_2)\cdot\text{H}_2\text{O}]^+$ ,  $[\text{Pt}(\text{C}_2\text{H}_4)\cdot\text{H}_2\text{O}]^+$ ,  $[\text{Pt}(\text{C}_2\text{H}_2)(\text{C}_2\text{H}_4)]^+$ , and  $[\text{Pt}(\text{C}_2\text{H}_4)_2]^+$  species (Table S1). Similarly, five new mass peaks appear when propane is introduced:  $[\text{Pt}(\text{C}_3\text{H}_4)]^+$ ,  $[\text{Pt}(\text{C}_3\text{H}_6)]^+$ ,  $[\text{Pt}(\text{C}_3\text{H}_4)_2]^+$ ,  $[\text{Pt}(\text{C}_3\text{H}_4)(\text{C}_3\text{H}_6)]^+$ , and  $[\text{Pt}(\text{C}_3\text{H}_6)_2]^+$  species (Figure 2e and Table S1). No other species with larger mass is found (Figures S4 and S5). Unlike the methane splitting over the  $\text{Pt}^+$  species, ethane and propane convert only to the corresponding  $[\text{Pt} + \text{alkene}]^+$  (where alkene includes ethylene

and propylene) and  $[\text{Pt} + \text{alkynes}]^+$  (alkynes include acetylene and allylene) via the dehydrogenation reactions, with alkenes being the main products. The  $\text{Pt}^+$  cation can chemo-adsorb only two alkenes, which is different from the observation in the case of CO gas. All of the results suggest that the nonoxidative dehydrogenation of alkanes can be over  $\text{Pt}^+$  at room temperature.

Overall, the  $\text{Pt}^+$  cations can be in situ generated with high efficiency by 5 ns single-shot 193 nm laser dissociation of  $\text{Pt}_n$  cluster precursors, and the HRMS system is proved to be a powerful tool for the characterization of important alkane conversion products and intermediates. Comparison with previous work with laser-ablation metal cation source for gas-phase methane reaction,<sup>29,30</sup> more conversion intermediates and products can be feasibly detected due to the high detection speed and sensitivity of our HRMS system.

To gain better insight into the mechanisms of alkanes conversion by  $\text{Pt}^+$ , we further carried out a DFT study of the reaction pathways for the conversion of methane, ethane, and propane by  $\text{Pt}^+$  at the B3LYP-D3(BJ)/def2-TZCPPD level of theory.  $\text{Pt}^+$  was set at its ground state, as indicated by the experimental results. Figure 3a shows the reaction energy diagram of methane conversion over  $\text{Pt}^+$  with optimized geometries of all of the reaction intermediates. Both  $[\text{Pt} + \text{ethylene}]^+$  and  $[\text{Pt} + \text{ethane}]^+$  products can be formed via the methylene reaction intermediates.  $[\text{Pt} + \text{ethane}]^+$  can also be produced through the cross-coupling of two  $\text{CH}_3$  species

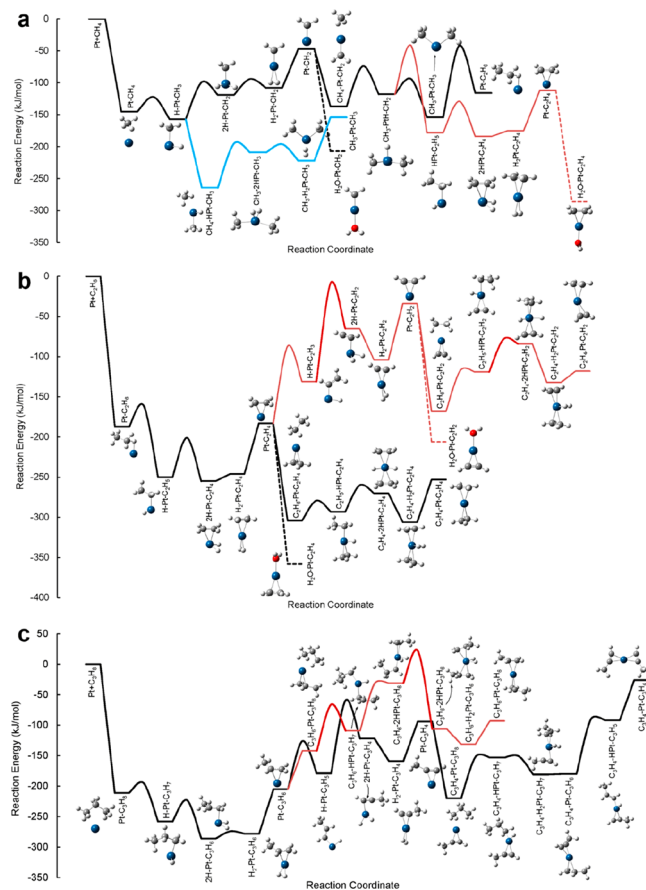


**Figure 3.** Reaction energy diagram of (a) methane, (b) ethane, and (c) propane dehydrogenation over  $\text{Pt}^+$  in the gas phase. Color code: Pt, blue; C, black; H, white; and O, red.

formed by the dehydrogenation of two methane molecules, although the “CH<sub>3</sub>” species is not detected by HRMS analysis. The formation of [Pt + ethylene]<sup>+</sup> is energetically more favorable than that of [Pt + ethane]<sup>+</sup>, and the presence of a trace amount of water (less than 15 ppm) could further stabilize the reaction intermediate of [Pt + methylene]<sup>+</sup> and the product of [Pt + C<sub>2</sub>H<sub>4</sub>]<sup>+</sup>, which is in good agreement with the experimental observations.

The mechanism of ethane dehydrogenation is demonstrated in Figure 3b. The dehydrogenation of the first ethane can first produce one ethylene over the Pt<sup>+</sup> cation, from which it can either adsorb and convert another ethane molecule to produce two ethylene molecules ([Pt(C<sub>2</sub>H<sub>4</sub>)<sub>2</sub>]<sup>+</sup>) or proceed with a further dehydrogenation reaction to give acetylene ([Pt-(C<sub>2</sub>H<sub>2</sub>)]<sup>+</sup>). The [Pt(C<sub>2</sub>H<sub>2</sub>)(C<sub>2</sub>H<sub>4</sub>)]<sup>+</sup> complex can then be formed via dehydrogenation of the second ethane over the so-formed [Pt(C<sub>2</sub>H<sub>2</sub>)]<sup>+</sup> intermediate. It is identified that the [Pt(C<sub>2</sub>H<sub>4</sub>)<sub>2</sub>]<sup>+</sup> formation pathway is the dominant reaction channel compared to the formation of [Pt(C<sub>2</sub>H<sub>2</sub>)(C<sub>2</sub>H<sub>4</sub>)]<sup>+</sup>. It is worth noting that the [Pt(C<sub>2</sub>H<sub>2</sub>)]<sup>+</sup> and [Pt(C<sub>2</sub>H<sub>4</sub>)]<sup>+</sup> species can be dramatically stabilized by the presence of water.

Figure 3c shows the reaction mechanism of propane dehydrogenation over the Pt<sup>+</sup> cation, which is a similar process to the case of ethane dehydrogenation. We investigated the conversion of two propane molecules toward different potential products of [Pt + propylene]<sup>+</sup> and [Pt + allylene]<sup>+</sup> as well and found that the formation of a mixture of propylene and allylene over the Pt<sup>+</sup> cation ([Pt(C<sub>3</sub>H<sub>4</sub>)(C<sub>3</sub>H<sub>6</sub>)]<sup>+</sup>) is energetically preferable to the synchronous production of two propylenes ([Pt(C<sub>3</sub>H<sub>6</sub>)<sub>2</sub>]<sup>+</sup>) or two allylenes ([Pt(C<sub>3</sub>H<sub>4</sub>)<sub>2</sub>]<sup>+</sup>), although the [Pt(C<sub>3</sub>H<sub>6</sub>)]<sup>+</sup> complex is relatively more stable compared to [Pt(C<sub>3</sub>H<sub>4</sub>)]<sup>+</sup>. These DFT results match well with the reported literature.<sup>31</sup> Therefore, these reaction mechanism results provide additional theoretical understandings and explanations for experimental in situ HRMS observations and propose plausible reaction pathways for various [Pt + alkene]<sup>+</sup> formation from light alkanes over the Pt<sup>+</sup> cations.

In conclusion, we constructed an ultraviolet laser–HRMS system for high-throughput Pt<sup>+</sup> cation generation and alkane conversion monitoring. The Pt<sup>+</sup> cation is generated by the 193 nm laser in situ dissociation of ligand-protected Pt clusters with high efficiency, which is much more convenient than the previous laser-ablation metal cation source. Furthermore, the orbitrap HRMS is demonstrated to be a powerful system for Pt<sup>+</sup> intermediates and product characterization due to its high detection speed and high mass resolution. We believe that the ultraviolet laser–HRMS system can play important roles in different types of metal cation generation and reaction profiling in the future, and these findings will enrich nanotechnology and nanoscience beyond the field of metal clusters in the gas phase.

## ■ ASSOCIATED CONTENT

### Supporting Information

The Supporting Information is available free of charge at <https://pubs.acs.org/doi/10.1021/acs.jpcllett.0c01416>.

Experimental procedures and DFT simulation; construction of the ultraviolet laser dissociation high-resolution mass spectrometry platform; full mass spectrum of a ligand-protected Pt cluster and the laser-dissociated Pt<sup>+</sup> cations; in-situ mass monitoring of the reaction profiling of the single Pt<sub>1</sub> in the presence of

methane, ethane, and propane and their corresponding pathways; observed and calculated mass of product ions; and coordinates and zero-point-corrected energies for all reaction intermediates and transition states (PDF)

## ■ AUTHOR INFORMATION

### Corresponding Authors

**Chunlei Xiao** – State Key Laboratory of Molecular Reaction Dynamics, Dalian Institute of Chemical Physics, Dalian 116023, China; [orcid.org/0000-0002-1549-5945](https://orcid.org/0000-0002-1549-5945); Email: [chunleixiao@dicp.ac.cn](mailto:chunleixiao@dicp.ac.cn)

**Fanjun Wang** – CAS Key Laboratory of Separation Sciences for Analytical Chemistry, Dalian Institute of Chemical Physics, Dalian 116023, China; University of Chinese Academy of Sciences, Beijing 100049, China; [orcid.org/0000-0002-8118-7019](https://orcid.org/0000-0002-8118-7019); Email: [wangfj@dicp.ac.cn](mailto:wangfj@dicp.ac.cn)

**Gao Li** – State Key Laboratory of Catalysis, Dalian Institute of Chemical Physics, Dalian 116023, China; University of Chinese Academy of Sciences, Beijing 100049, China; [orcid.org/0000-0001-6649-5796](https://orcid.org/0000-0001-6649-5796); Email: [gaoli@dicp.ac.cn](mailto:gaoli@dicp.ac.cn)

### Authors

**Zheyi Liu** – CAS Key Laboratory of Separation Sciences for Analytical Chemistry, Dalian Institute of Chemical Physics, Dalian 116023, China

**Zhimin Li** – State Key Laboratory of Catalysis, Dalian Institute of Chemical Physics, Dalian 116023, China; University of Chinese Academy of Sciences, Beijing 100049, China

**Guanna Li** – Inorganic Systems Engineering, Department of Chemical Engineering, Delft University of Technology, 2629, HZ, Delft, The Netherlands; [orcid.org/0000-0003-3031-8119](https://orcid.org/0000-0003-3031-8119)

**Zhipeng Wang** – State Key Laboratory of Molecular Reaction Dynamics, Dalian Institute of Chemical Physics, Dalian 116023, China

**Can Lai** – CAS Key Laboratory of Separation Sciences for Analytical Chemistry, Dalian Institute of Chemical Physics, Dalian 116023, China

**Xiaolei Wang** – CAS Key Laboratory of Separation Sciences for Analytical Chemistry and State Key Laboratory of Molecular Reaction Dynamics, Dalian Institute of Chemical Physics, Dalian 116023, China

**Evgeny A. Pidko** – Inorganic Systems Engineering, Department of Chemical Engineering, Delft University of Technology, 2629, HZ, Delft, The Netherlands; [orcid.org/0000-0001-9242-9901](https://orcid.org/0000-0001-9242-9901)

**Xueming Yang** – State Key Laboratory of Molecular Reaction Dynamics, Dalian Institute of Chemical Physics, Dalian 116023, China; [orcid.org/0000-0001-6684-9187](https://orcid.org/0000-0001-6684-9187)

Complete contact information is available at: <https://pubs.acs.org/doi/10.1021/acs.jpcllett.0c01416>

### Author Contributions

#Z.L., Z.L., and G.L. contributed equally.

### Notes

The authors declare no competing financial interest.

## ■ ACKNOWLEDGMENTS

We acknowledge the financial support of the National Key R&D Program of China (2016YFF0200504), the National Natural Science Foundation of China (nos. 91853101 and 21675152), the Original Innovation Project of CAS (ZDBS-

LY-SLH032), the Liaoning Revitalization Talents Program (XLYC1807121), and the grant of CAS (GJJSTD20190002) and a grant from DICP (ZZBS201603). We also acknowledge the technological support from the Dalian Coherent Light Source. Guanna Li thanks the Dutch Organization for Scientific Research (NWO) for financial support through her personal Veni grant (no. 016.Veni.172.034) and for access to the SURFsara supercomputer facilities.

## REFERENCES

- (1) Amghizar, I.; Vandewalle, L. A.; Van Geem, K. M.; Marin, G. B. New trends in olefin production. *Engineering* **2017**, *3*, 171–178.
- (2) Schröder, D.; Schwarz, H. Gas-phase activation of methane by ligated transition-metal cations. *Proc. Natl. Acad. Sci. U. S. A.* **2008**, *105*, 18114–18119.
- (3) Trevor, D. J.; Cox, D. M.; Kaldor, A. Methane activation on unsupported platinum clusters. *J. Am. Chem. Soc.* **1990**, *112*, 3742–3749.
- (4) Wesendrup, R.; Schröder, D.; Schwarz, H. Catalytic Pt<sup>+</sup>-mediated oxidation of methane by molecular oxygen in the gas phase. *Angew. Chem., Int. Ed. Engl.* **1994**, *33*, 1174–1176.
- (5) Wesendrup, R.; Schwarz, H. Tantalum-mediated coupling of methane and carbon dioxide in the gas phase. *Angew. Chem., Int. Ed. Engl.* **1995**, *34*, 2033–2035.
- (6) Rettner, C. T.; Pfnür, H. E.; Auerbach, D. J. On the role of vibrational energy in the activated dissociative chemisorption of methane on tungsten and rhodium. *J. Chem. Phys.* **1986**, *84*, 4163–4167.
- (7) Wheeler, O. W.; Salem, M.; Gao, A.; Bakker, J. M.; Armentrout, P. B. Activation of C-H bonds in Pt<sup>+</sup> + x CH<sub>4</sub> Reactions, where x = 1–4: Identification of the platinum dimethyl cation. *J. Phys. Chem. A* **2016**, *120*, 6216–6227.
- (8) Pavlov, M.; Blomberg, M. R. A.; Siegbahn, P. E. M.; Wesendrup, R.; Heinemann, C.; Schwarz, H. Pt<sup>+</sup>-catalyzed oxidation of methane: Theory and experiment. *J. Phys. Chem. A* **1997**, *101*, 1567–1579.
- (9) Kummerlöwe, G.; Balteanu, I.; Sun, Z.; Balaj, O. P.; Bondybey, V. E.; Beyer, M. K. Activation of methane and methane-d4 by ionic platinum clusters. *Int. J. Mass Spectrom.* **2006**, *254*, 183–188.
- (10) Cox, R. M.; Armentrout, P. B.; de Jong, W. A. Activation of CH<sub>4</sub> by Th<sup>+</sup> as studied by guided ion beam mass spectrometry and quantum chemistry. *Inorg. Chem.* **2015**, *54*, 3584–3599.
- (11) Armentrout, P.; Parke, L.; Hinton, C.; Citir, M. Activation of methane by Os<sup>+</sup>: Guided-ion-beam and theoretical studies. *Chem-PlusChem* **2013**, *78*, 1157–1173.
- (12) Maruyama, S.; Anderson, L. R.; Smalley, R. E. Direct injection supersonic cluster beam source for FT-ICR studies of clusters. *Rev. Sci. Instrum.* **1990**, *61*, 3686–3693.
- (13) Luo, Z.; Castleman, A. W.; Khanna, S. N. Reactivity of metal clusters. *Chem. Rev.* **2016**, *116*, 14456–14492.
- (14) Hada, M.; Nakatsuji, H.; Nakai, H.; Gyobu, S.; Miki, S. Theoretical study on the methane activation reactions by Pt, Pt<sup>+</sup>, and Pt<sup>-</sup> atoms. *J. Mol. Struct.: THEOCHEM* **1993**, *281*, 207–212.
- (15) Lapoutre, V. J.; Redlich, B.; van der Meer, A. F.; Oomens, J.; Bakker, J. M.; Sweeney, A.; Mookherjee, A.; Armentrout, P. B. Structures of the dehydrogenation products of methane activation by 5d transition metal cations. *J. Phys. Chem. A* **2013**, *117*, 4115–4126.
- (16) Irikura, K. K.; Beauchamp, J. Electronic structure considerations for methane activation by third-row transition-metal ions. *J. Phys. Chem.* **1991**, *95*, 8344–8351.
- (17) Heinemann, C.; Wesendrup, R.; Schwarz, H. Pt<sup>+</sup>-mediated activation of methane: theory and experiment. *Chem. Phys. Lett.* **1995**, *239*, 75–83.
- (18) Zheng, K.; Zhang, J.; Zhao, D.; Yang, Y.; Li, Z.; Li, G. Motif mediated Au<sub>25</sub>(SPh)<sub>5</sub>(PPh<sub>3</sub>)<sub>10</sub>X<sub>2</sub> nanorod of conjugated electron delocalization. *Nano Res.* **2019**, *12*, 501–507.
- (19) Neumaier, M.; Weigend, F.; Hampe, O.; Kappes, M. M. Reactions of mixed silver-gold cluster cations Ag<sub>m</sub>Au<sub>n</sub><sup>+</sup> (m+n = 4,5,6) with CO: radiative association kinetics and density functional theory computations. *J. Chem. Phys.* **2006**, *125*, 104308.
- (20) Black, D. M.; Robles, G.; Lopez, P.; Bach, S. B. H.; Alvarez, M.; Whetten, R. L. Liquid chromatography separation and mass spectrometry detection of silver-lipoate Ag<sub>29</sub>(LA)<sub>12</sub> nanoclusters: Evidence of isomerism in the solution phase. *Anal. Chem.* **2018**, *90*, 2010–2017.
- (21) Maity, P.; Takano, S.; Yamazoe, S.; Wakabayashi, T.; Tsukuda, T. Binding motif of terminal alkynes on gold clusters. *J. Am. Chem. Soc.* **2013**, *135*, 9450–9457.
- (22) Liu, C.; Yan, C.; Lin, J.; Yu, C.; Huang, J.; Li, G. One-pot synthesis of Au<sub>144</sub>(SCH<sub>2</sub>Ph)<sub>60</sub> nanoclusters and catalytic application. *J. Mater. Chem. A* **2015**, *3*, 20167–20173.
- (23) Brodbelt, J. S.; Morrison, L. J.; Santos, I. Ultraviolet photodissociation mass spectrometry for analysis of biological molecules. *Chem. Rev.* **2020**, *120*, 3328–3380.
- (24) Fort, K. L.; Dyachenko, A.; Potel, C. M.; Corradini, E.; Marino, F.; Barendregt, A.; Makarov, A. A.; Scheltema, R. A.; Heck, A. J. Implementation of ultraviolet photodissociation on a Benchtop Q exactive mass spectrometer and its application to phosphoproteomics. *Anal. Chem.* **2016**, *88*, 2303–2310.
- (25) Mehaffey, M. R.; Schardon, C. L.; Novelli, E. T.; Cammarata, M. B.; Webb, L. J.; Fast, W.; Brodbelt, J. S. Investigation of GTP-dependent dimerization of G12X K-Ras variants using ultraviolet photodissociation mass spectrometry. *Chem. Sci.* **2019**, *10*, 8025–8034.
- (26) Greisch, J.-F.; Tamara, S.; Scheltema, R. A.; Maxwell, H. W. R.; Fagerlund, R. D.; Fineran, P. C.; Tetter, S.; Hilvert, D.; Heck, A. J. R. Expanding the mass range for UVPD-based native top-down mass spectrometry. *Chem. Sci.* **2019**, *10*, 7163–7171.
- (27) Liu, C.; Li, G.; Kauffman, D. R.; Pang, G.; Jin, R. Synthesis of ultrasmall platinum nanoparticles and structural relaxation. *J. Colloid Interface Sci.* **2014**, *423*, 123–128.
- (28) Shuman, N. S.; Ard, S. G.; Sweeny, B. C.; Pan, H.; Viggiano, A. A.; Keyes, N. R.; Guo, H.; Owen, C. J.; Armentrout, P. B. Au<sup>2+</sup> cannot catalyze conversion of methane to ethene at low temperature. *Catal. Sci. Technol.* **2019**, *9*, 2767–2780.
- (29) Perera, M.; Metz, R. B.; Kostko, O.; Ahmed, M. Vacuum ultraviolet photoionization studies of PtCH<sub>2</sub> and H-Pt-CH<sub>3</sub>: A potential energy surface for the Pt+ CH<sub>4</sub> reaction. *Angew. Chem., Int. Ed.* **2013**, *52*, 888–891.
- (30) Harding, D. J.; Kerpel, C.; Meijer, G.; Fielicke, A. Activated methane on small cationic platinum clusters. *Angew. Chem., Int. Ed.* **2012**, *51*, 817–819.
- (31) Yang, M.-L.; Zhu, Y.-A.; Fan, C.; Sui, Z.-J.; Chen, D.; Zhou, X.-G. DFT study of propane dehydrogenation on Pt catalyst: effects of step sites. *Phys. Chem. Chem. Phys.* **2011**, *13*, 3257–3267.